Available online at www.sciencedirect.com

SciVerse ScienceDirect

Ceramics International 38 (2012) 6229–6234

CERAMICS INTERNATIONAL

www.elsevier.com/locate/ceramint

Two-step sintering of aluminum-doped zinc oxide sputtering target by using a submicrometer zinc oxide powder

Ming-Wei Wu

National Formosa University, Department of Materials Science and Engineering, No.64, Wunhua Rd., Huwei Township, Yunlin County 63201, Taiwan, ROC

Received 9 February 2012; received in revised form 18 April 2012; accepted 27 April 2012
Available online 11 May 2012

Abstract

Aluminum-doped zinc oxide (AZO) is a potential substitute for tin-doped indium oxide due to its versatility. The properties of AZO films are related to those of the AZO sputtering target. To improve the performances of AZO targets, two-step sintering was used to densify a submicrometer zinc oxide (ZnO) powder with a size of 0.4 μm to produce both AZO and ZnO targets.

The results showed that the submicrometer ZnO powder cannot be densified by two-step sintering due to its coarse particle size and hexagonal structure. However, a 2 wt% additive of Al_2O_3 in ZnO can modify the kinetic window of two-step sintering and help in the densification. Using two-step sintering, the sintered density of the AZO target can be improved from 97.4% to 99.8%. The grain size is also reduced by 60%, from 9.1 μm to 3.6 μm.

Keywords: AZO; Two-step sintering; Grain size; Microstructure-final

1. Introduction

Transparent conductive oxide (TCO) films, particularly tin-doped indium oxide (ITO) ones, have been applied in liquid crystal displays, solar cells, and other devices as the transparent conductive electrode for several decades. However, the alternatives to ITO have been extensively developed due to the shortage and high cost of indium. Zinc oxide (ZnO) with an addition of 2 wt% Al_2O_3 (aluminum-doped zinc oxide, AZO) is regarded as a potential substitute for ITO due to its versatility [1–3]. Among the deposition techniques of AZO and other TCO films, magnetron sputtering is a versatile method and is applied widely. The sputtering targets apparently affect the performances of various thin films and are thus the key material required [4–9].

Because the sputtering targets are indispensable for sputtering, the importance of targets on the performances of various thin films has recently been investigated [4–10]. Nodule formation during sputtering is related to the pores in the targets and increases particulate contamination, which deteriorates the quality of the films sputtered [9,10]. A higher target density also enhances deposition rate [9]. Thus, the processes and the properties of AZO targets have been recently investigated in some studies [4,11–15]. Those studies focused mainly on the sintered density and the microstructure of the AZO target [12,14,15]. To attain an ultra-high sintered density, Chen et al. [16] proposed a novel sintering technique, two-step sintering (TSS), for achieving an almost fully dense ceramic while inhibiting exaggerated grain growth. This versatile technique has been successfully used in Y_2O_3 [16,17], Al_2O_3 [18–22], ZnO [23,24], ZrO_2 [21,22,25], $BaTiO_3$ [26], and TiO_2 [27] to fabricate fine-grain ceramics. This technique can also be applied in the sintering of both ZnO and SiC with the presence of liquid phase [24,28].

Most research on TSS has concentrated on the optimization of TSS parameters for a ceramic powder with a particular particle size and composition. However, few studies have examined the influences of the dopants on the TSS of ceramics [16,17,21]. For the TSS of Y_2O_3 powder, Chen et al. [16,17] indicated that an addition of 1 at% Mg or 1 at% Nb does not affect the feasibility of TSS, though the kinetic windows are shifted to lower and higher temperatures, respectively. Maca et al. [21] found that

E-mail address: mwwu@nfu.edu.tw

0272-8842/$36.00
http://dx.doi.org/10.1016/j.ceramint.2012.04.076

the achievement of TSS for 8Y-ZrO_2 is better than that for 3Y-ZrO_2. These studies demonstrated that the role of the dopant cannot be neglected in TSS. Furthermore, most studies have used nanometer powders as the raw materials for two-step sintering [16,17,21–28]. However, nanometer powders are less likely to be well dispersed and are very expensive. The hazard to the human body is also a key issue. These drawbacks prohibit the wide application of nanometer powders. Recently, some researchers have used a submicrometer Al_2O_3 powder with a particle size of 0.15 μm to successfully produce high-density Al_2O_3 ceramics with a submicrometer grain size by TSS, though the grain growth cannot be inhibited completely [18,19,21]. In contrast, Michálková et al. [29] used an identical submicrometer Al_2O_3 powder and found that the sintering trajectories of the two-step sintered specimens are similar to those of the conventional sintered ones, even with modifications to the forming procedures. No microstructure refinement was found in the two-sintering regime. For TSS, these above studies have shown that the feasibility of submicrometer powders is quite complex and is still undetermined.

In our previous study, both AZO and ZnO sputtering targets were produced with a submicrometer ZnO powder. The densification, microstructure, and electrical properties of these targets that were sintered by conventional sintering (CS) were studied [11]. To further improve the performances of both AZO and ZnO targets, this study investigated the influence of TSS on the densification and microstructure of these targets. The effects of 2 wt% Al_2O_3 addition on the TSS of ZnO target were also studied and are discussed.

2. Experimental procedure

ZnO and Al_2O_3 powder with median particle sizes of 0.4 μm and 0.2 μm, respectively, were used as the base powders in this study. To prepare the slurry of ZnO powder, 0.2 wt% dispersant of ammonium polyacrylate was first added to distilled water, and then the ZnO powder was added to the aqueous solution. For the slurry of AZO powder, 98 wt% ZnO and 2 wt% Al_2O_3 powders were added to the aqueous solution. The solid contents of both ZnO and AZO slurries were 35 vol%, which corresponded to 75 wt%. These two aqueous slurries were ball milled for 3 h with 2 mm-diameter ZrO_2 milling media. The ball to powder ratio was 3:1. Subsequently, 0.5 wt% binder of polyacrylic emulsion was added to the slurries, after which the slurries were ball milled for an additional 1 h. The amounts of the dispersant (0.2 wt%) and the binder (0.5 wt%) were based on the weight of dry powder. These two slurries were then spray-dried by hot air using a spray dryer (L-8, Ohkawara Kakohki Co., Yokohama, Japan). The median sizes (D_{50}) of ZnO and AZO spray-dried granules were about 30 μm.

The spray-dried granules were uniaxially compacted into a 13 mm-diameter and 6 mm-thick disk at a pressure of 150 MPa. The green densities of both ZnO and AZO compacts ranged from 61% to 62%. For TSS, the green compacts were first heated at 10 °C/min to T_1, the peak sintering temperature, and then immediately cooled at 50 °C/min to T_2, the soaking temperature. The soaking time at T_2 was 12 h. The temperatures of T_2 selected were lower than those of T_1 by 50 °C, 150 °C, and 250 °C. The green compacts were also sintered by CS for comparison. The sintering temperatures of CS ranged from 1000 °C to 1500 °C and the soaking time was 12 h. The sintered densities of the two-step sintered and conventional sintered specimens were measured using the Archimedes method in distilled water. The theoretical densities of ZnO and Al_2O_3 were taken as 5.67 g/cm^3 and 3.98 g/cm^3, respectively. The theoretical density of AZO was thus assumed to be 5.64 g/cm^3. To observe the microstructure, the fracture surfaces of the sintered specimens were thermally etched at 950 °C for 1 h and then examined under a scanning electron microscope (JSM-6360, JEOL, Tokyo, Japan). The average grain sizes of both ZnO and AZO targets were calculated [30].

3. Results and discussion

3.1. Two-step sintering of ZnO

The sintered density and grain size of ZnO after TSS are shown in Table 1.The result showed that the highest sintered density of ZnO densified by TSS was only 95.1%. When T_1 and T_2 were further increased, the densification of ZnO could not be improved due to extensive evaporation and grain growth. The microstructures of ZnO after TSS also indicated inferior densification, as shown in Fig. 1. For comparison, the sintered density and grain size of ZnO after CS as a function of the sintering temperatures are also shown in Fig. 2. The results showed that, after sintering at 1200 °C, the highest sintered density of 97.3% was achieved. When the sintering temperature was higher than 1200 °C, the sintered density decreased slightly because ZnO apparently evaporated. The weight loss of ZnO increased from 0.9% to 7.7% as the

Table 1
The sintered density and grain size of ZnO after two-step sintering.

TSS program	T_1 (°C)	T_2 (°C)	Relative density (%)	Grain size (μm)
Z1	1000	950	93.8	3.4
Z2	1100	1050	95.1	3.9
Z3	1200	1150	94.4	7.8
Z4	1300	1250	95.1	12.0

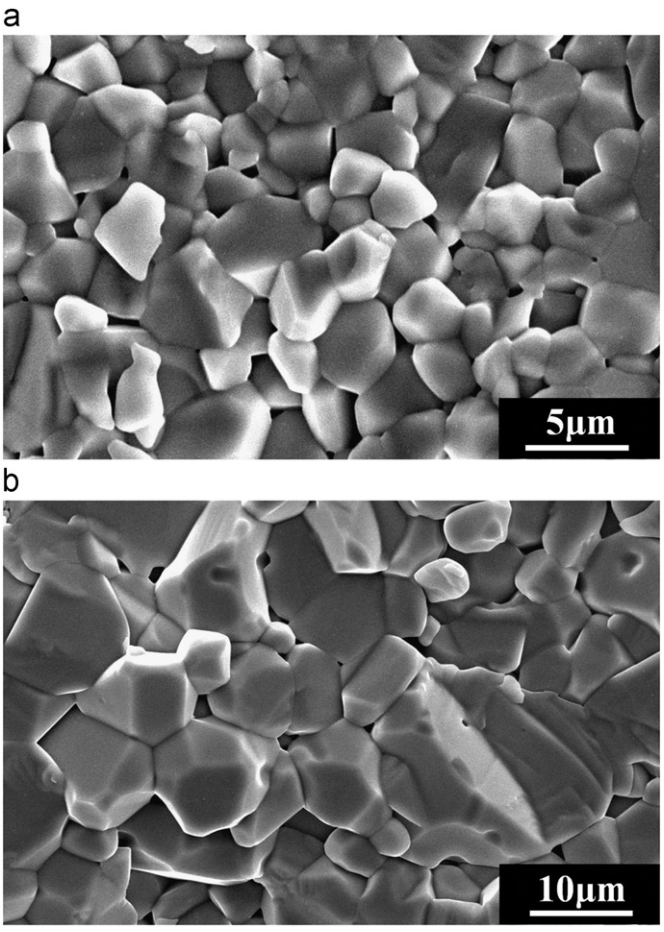

Fig. 1. The microstructures of ZnO targets densified by two-step sintering (a) Z2 program (T_1=1100 °C, T_2=1050 °C) and (b) Z4 program (T_1=1300 °C, T_2=1250 °C).

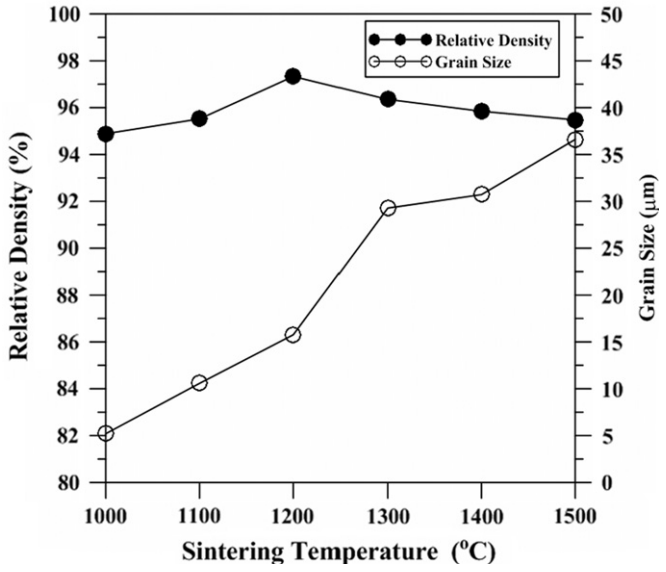

Fig. 2. The sintered densities and grain sizes of ZnO targets densified by conventional sintering as a function of the sintering temperatures.

sintering temperature was increased from 1200 °C to 1500 °C. Moreover, the grain growth of ZnO densified by CS was clearly found to be related to the sintering temperature. The grain sizes of ZnO that were sintered at 1000 °C and 1500 °C were 5.2 μm and 36.6 μm, respectively. Whether or not TSS or CS was used to densify the ZnO target, the results of this study indicated clearly that the ZnO powder with a size of 0.4 μm could not be densified to a density higher than 98%.

Maca et al. [21,22] previously investigated the effects of crystal structures on the TSS of the ceramics and showed that ceramics with cubic structures, including $SrTiO_3$ and 8 mol% Y_2O_3-doped ZrO_2, can be densified by TSS facilely, followed by those with hexagonal and tetragonal structures. The efficiency of TSS for oxide ceramics depends more on the crystal structure than on the particle size, compaction method, or microstructure of green body [21]. These authors also showed that an increase of Y_2O_3 from 3 mol% to 8 mol% changes the crystal structure of ZrO_2 from a tetragonal structure to a cubic one and leads to the success of two-step sintered ZrO_2 [21].

ZnO with a hexagonal wurtzite structure was investigated in this study. The efficiency of TSS for ZnO was presumed to be low. Mazaheri et al. [23] indicated that a nanometer ZnO powder with a particle size of 20–40 nm can be used to produce ZnO ceramic with a relative density of 98% and a grain size of 0.68 μm by TSS. T_1 and T_2 were selected as 800 °C and 750 °C, respectively. However, the grain growth of ZnO cannot be totally prohibited during TSS, even though the nanometer powder was used. Table 1 indicates that densifying the ZnO target by TSS did not succeed when the particle size of the ZnO powder used was 0.4 μm. Thus, the inefficiency of TSS on ZnO could be attributed to its coarse particle size and hexagonal structure.

3.2. Two-step sintering of AZO

Table 2 shows the sintered density and grain size of AZO after TSS. The results indicated that only A4 and A5 programs were beneficial for TSS and resulted in a sintered density higher than 99.0%. The microstructures of AZO densified by various TSS programs also supported this finding, as shown in Fig. 3. AZO could be densified by TSS when T_1 was 1500 °C. After the first step at 1500 °C, AZO must be immediately cooled to 1350 °C and 1450 °C and then soaked for 12 h. The sintered density achieved for soaking at 1350 °C was 99.8%, slightly higher than that for soaking at 1450 °C, 99.5%. The likely explanation was that extensive evaporation occurred at 1450 °C, and the final weight loss was 6.2 wt%. Furthermore, TSS was inactive as T_2 decreased from 1350 °C to 1250 °C, as shown in Table 2. The remaining A1 and A2 programs were also found to be ineffective for TSS of AZO. For comparison, Fig. 4 shows the sintered densities and grain sizes of AZO targets after CS as a function of the sintering temperatures. The sintered density of AZO densified by CS increased with the sintering temperatures. After sintering at 1500 °C for 12 h, the highest sintered density of AZO was achieved,

Table 2
The sintered density and grain size of AZO after two-step sintering.

TSS program	T_1 (°C)	T_2 (°C)	Relative density (%)	Grain size (μm)
A1	1400	1350	96.8	3.3
A2	1450	1400	97.9	4.6
A3	1500	1250	97.9	3.2
A4	1500	1350	99.8	3.6
A5	1500	1450	99.5	4.7

97.4%. These results indicated that the sintered density of AZO densified by CS could not be higher than 98% when the submicrometer ZnO powder was used. Moreover, the grain size ranged from 1.7 μm to 9.1 μm. The grain size obviously increased from 4.0 μm to 9.1 μm as the sintering temperature was increased from 1400 °C to 1500 °C.

To further compare the densifications of AZO densified by both TSS and CS, the sintering trajectories of AZO are demonstrated in Fig. 5. After CS at 1500 °C and soaking for 12 h, the sintered density and grain size of the AZO target were 97.4% and 9.1 μm, respectively. However, after TSS under the A4 program (T_1=1500 °C, T_2=1350 °C), the sintered density and grain size of the AZO target could be improved to 99.8% and 3.6 μm, respectively. The sintering trajectories clearly demonstrated that TSS resulted in greater densification and slower grain growth of AZO than CS did, as shown in Fig. 5.

3.3. The effect of Al_2O_3 additive

The preceding results clearly showed that the addition of 2 wt% Al_2O_3 played a decisive role in the TSS of the ZnO target. ZnO could not be successfully densified by TSS when the ZnO powder with a particle size of 0.4 μm was used. In contrast, the addition of 2 wt% Al_2O_3 in ZnO helped in the densification and suppressed the grain growth during TSS. For the densification of the ceramics using TSS, the prerequisite is that sintered density after the first step at T_1 must exceed a critical relative density [16]. The critical relative density has been reported to be from about 73% to 92%, depending on the material, particle size, and compaction method [16–20,23,25,26,28]. To clarify the critical density for TSS of AZO in this study, the sintered densities after the first step were also measured. The sintered densities after the first step at 1400 °C, 1450 °C, and 1500 °C were 96.3%, 96.6%, and 97.7%, respectively. This result demonstrated that the critical density for AZO was as high as 97.7%, which was much higher than those of other studies [16–20,23,25,26,28]. This high critical density was due not only to the coarse powder used but also the hexagonal structure and the compaction method applied. However, in the case of ZnO, the sintered densities after the first step at 1100 °C, 1200 °C, and 1300 °C were only 94.8%, 94.7%, and 95.6%, respectively, and did not approach 98%.

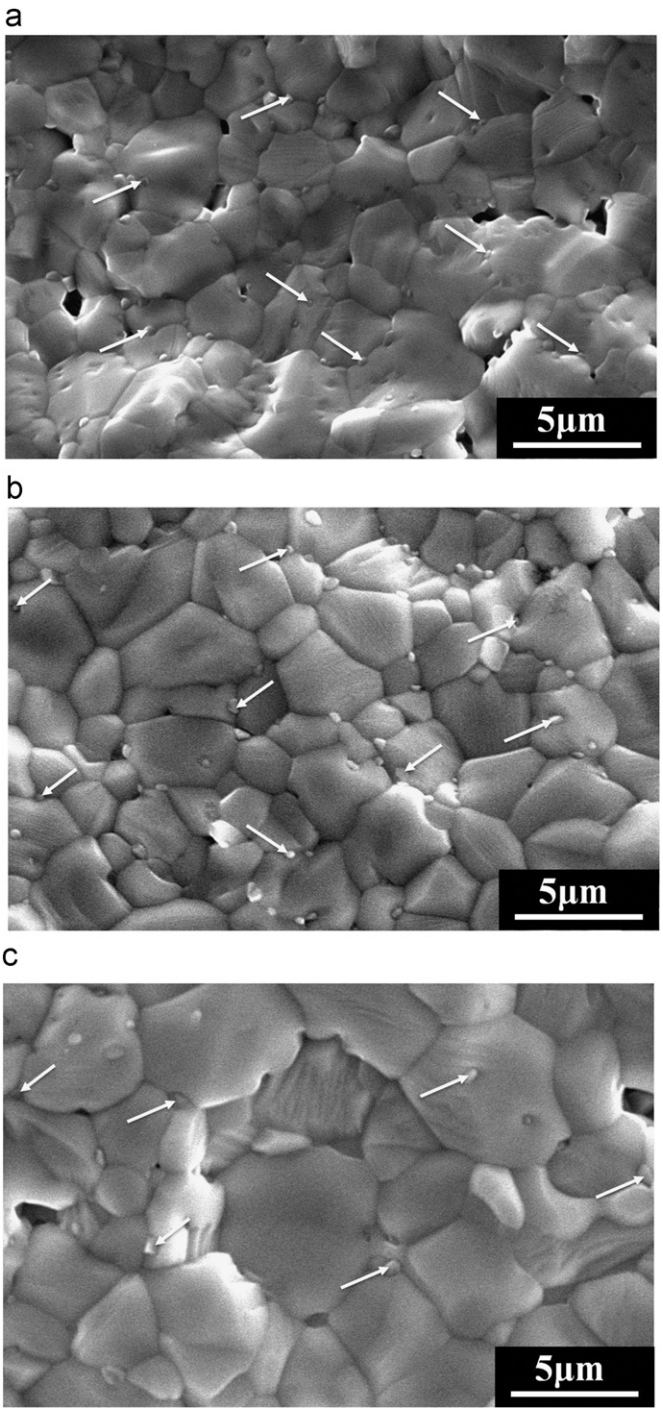

Fig. 3. The microstructures of AZO targets densified by two-step sintering (a) A3 program (T_1=1500 °C, T_2=1250 °C), (b) A4 program (T_1=1500 °C, T_2=1350 °C), and (c) A5 program (T_1=1500 °C, T_2=1450 °C).

The effects of Al_2O_3 addition on TSS of ZnO cannot be simply attributed to the difference between the crystal structures of AZO and ZnO. Some studies [4,11,12] have shown that the addition of 2 wt% Al_2O_3 additive does not result in the phase transformation of ZnO. Al_2O_3 reacts with ZnO to form $ZnAl_2O_4$ spinel precipitates during heating. These $ZnAl_2O_4$ precipitates were also found in the microstructure of two-step sintered AZO, as indicated by the white

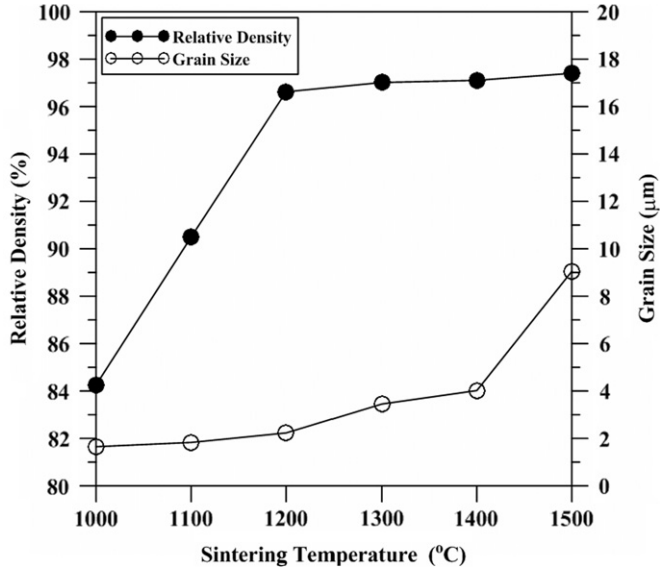

Fig. 4. The sintered densities and grain sizes of AZO targets densified by conventional sintering as a function of the sintering temperatures.

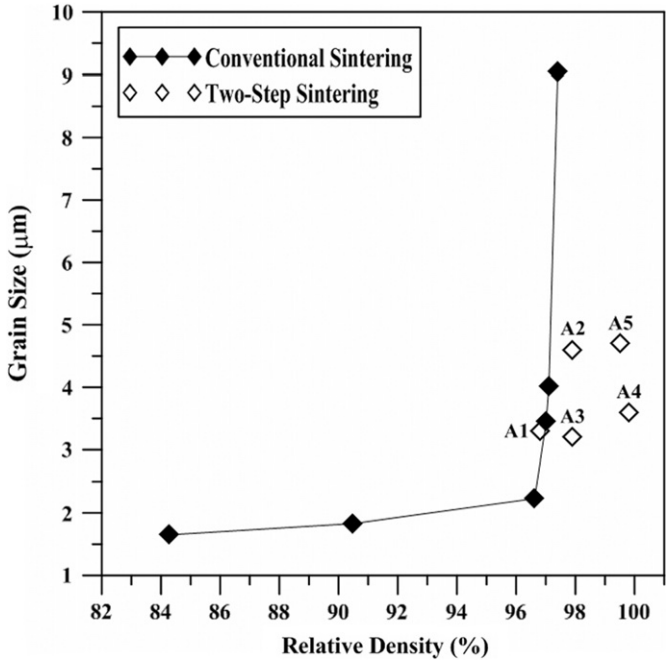

Fig. 5. The sintering trajectories of AZO targets densified by conventional sintering and two-step sintering.

arrows in Fig. 3. These precipitates can drag the grain boundary and contribute to a higher sintered density and a finer grain size of AZO [11,31]. The densification and sintered density of AZO was higher than those of ZnO when the sintering temperature was higher than 1300 °C, as can be seen from comparing Figs. 2 and 4. Thus, the critical relative density of AZO, 97.7%, could be achieved after the first step at 1500 °C.

Previous studies [18,19,21] indicated that an Al_2O_3 powder with a particle size of 0.15 μm and a hexagonal structure can be densified by TSS. Based on the results of this study, it is concluded that the ZnO powder used in this study cannot be densified by TSS due to its coarse particle size and hexagonal structure. However, the 2 wt% Al_2O_3 additive can sufficiently affect the densification behavior of two-step sintered ZnO and achieve a sintered density higher than 99.5%, though the kinetic window is still narrow. The influences of various additives on two-step sintered ceramics should be further clarified.

4. Conclusions

To improve the performances of both AZO and ZnO sputtering targets produced by a submicrometer ZnO powder with a size of 0.4 μm, two-step sintering was used to optimize the sintered density and grain size. The findings can be summarized as follows.

1. The submicrometer ZnO powder cannot be densified by two-step sintering due to its coarse particle size and hexagonal structure.
2. The densification of an AZO target can be enhanced by two-step sintering. The 2 wt% Al_2O_3 additive in ZnO is beneficial to maintaining the kinetic window of two-step sintering and, thus, to the densification.
3. With adequate parameters of two-step sintering, the sintered density of the AZO target can be improved from 97.4% to 99.8%. The grain size can also be reduced from 9.1 μm to 3.6 μm.

Acknowledgment

The authors thank the National Science Council of the Republic of China for their support of this project under contract number NSC 99–2218-E-150-046.

References

[1] T. Minami, Substitution of transparent conducting oxide thin films for indium tin oxide transparent electrode applications, Thin Solid Films 516 (2008) 1314–1321.
[2] G. Fang, D. Li, B.L. Yao, Fabrication and vacuum annealing of transparent conductive AZO thin films prepared by DC magnetron sputtering, Vacuum 68 (2003) 363–372.
[3] W. Dewald, V. Sittinger, W. Werner, C. Jacobs, B. Szyszka, Optimization of process parameters for sputtering of ceramic ZnO:Al_2O_3 targets for a-Si:H/μc-Si:H solar cells, Thin Solid Films 518 (2009) 1085–1090.
[4] H.S. Huang, H.C. Tung, C.H. Chiu, I.T. Hong, R.Z. Chen, J.T. Chang, H.K. Lin, Highly conductive alumina-added ZnO ceramic target prepared by reduction sintering and its effect on the properties of deposited thin films by direct current magnetron sputtering, Thin Solid Films 518 (2010) 6071–6075.
[5] T. Minami, J.I. Oda, J.I. Nomoto, T. Miyata, Effect of target properties on transparent conducting impurity-doped ZnO thin films deposited by DC magnetron sputtering, Thin Solid Films 519 (2010) 385–390.

[6] K.L. Ying, T.E. Hsieh, Y.F. Hsieh, Colloidal dispersion of nano-scale ZnO powders using amphibious and anionic polyelectrolytes, Ceramics International 35 (2009) 1165–1171.
[7] K. Nakashima, Y. Kumahara, Effect of tin oxide dispersion on nodule formation in ITO sputtering, Vacuum 66 (2002) 221–226.
[8] J. Sarkar, P. McDonald, P. Gilman, Surface characteristics of titanium targets and their relevance to sputtering performance, Thin Solid Films 517 (2009) 1970–1976.
[9] B.L. Gehman, S. Jonsson, T. Rudolph, M. Sherer, M. Weigert, R. Werner, Influence of manufacturing process of indium tin oxide sputtering targets on sputtering behavior, Thin Solid Films 220 (1992) 333–336.
[10] C.F. Lo, D. Draper, Quantitative measurement of nodule formation in W-Ti sputtering, Journal of Vacuum Science and Technology A 16 (1998) 2418–2422.
[11] M.W. Wu, D.S. Liu, Y.H. Su, The densification, microstructure, and electrical properties of aluminum-doped zinc oxide sputtering target for transparent conductive oxide film, Journal of the European Ceramic Society, http://dx.doi.org/10.1016/j.jeurceramsoc.2012.04.030, in press.
[12] Y.H. Sun, W.H. Xiong, C.H. Li, L. Yuan, Effect of dispersant concentration on preparation of an ultrahigh density ZnO–Al_2O_3 target by slip casting, Journal of the American Ceramic Society 92 (2009) 2168–2171.
[13] C.P. Liu, G.R. Jeng, Properties of aluminum doped zinc oxide materials and sputtering thin films, Journal of Alloys and Compounds 468 (2009) 343–349.
[14] J. Zhang, W. Zhang, E. Zhao, H.J. Jacques, Study of high-density AZO ceramic target, Materials Science in Semiconductor Processing 14 (2011) 189–192.
[15] B. Hwang, Y.K. Paek, S.H. Yang, S. Lim, W.S. Seo, K.S. Oh, Densification of Al-doped ZnO via preliminary heat treatment under external pressure, Journal of Alloys and Compounds 509 (2011) 7478–7483.
[16] I.W. Chen, X.H. Wang, Sintering dense nanocrystalline ceramics without final-stage grain growth, Nature 404 (2000) 168–171.
[17] X.H. Wang, P.L. Chen, I.W. Chen, Two-step sintering of ceramics with constant grain-size, I. Y_2O_3, Journal of the American Ceramic Society 89 (2006) 431–437.
[18] Z.R. Hesabi, M. Haghighatzadeh, M. Mazaheri, D. Galusek, S.K. Sadrnezhaad, Suppression of grain growth in sub-micrometer alumina via two-step sintering method, Journal of the European Ceramic Society 29 (2009) 1371–1377.
[19] K. Bodišová, P. Šajgalík, Two-stage sintering of alumina with submicrometer grain size, Journal of the American Ceramic Society 90 (2007) 330–332.
[20] C.J. Wang, C.Y. Huang, Y.C. Wu, Two-step sintering of fine alumina–zirconia ceramics, Ceramics International. 35 (2009) 1467–1472.
[21] K. Maca, V. Pouchly, P. Zalud, Two-step sintering of oxide ceramics with various crystal structures, Journal of the European Ceramic Society 30 (2010) 583–589.
[22] K. Maca, V. Pouchly, Z. Shen, Two-step sintering and spark plasma sintering of Al_2O_3, ZrO_2, and $SrTiO_3$ ceramics, Integrated Ferroelectrics 99 (2008) 114–124.
[23] M. Mazaheri, A.M. Zahedi, S.K. Sadrnezhaad, Two-step sintering of nanocrystalline ZnO compacts-effect of temperature on densification and grain growth, Journal of the American Ceramic Society 91 (2008) 56–63.
[24] P. Durán, J. Tartaj, C. Moure, Fully dense, fine-grained, doped zinc oxide varistors with improved nonlinear properties by thermal processing optimization, Journal of the American Ceramic Society 86 (2003) 1326–1329.
[25] M. Mazaheri, M. Valefi, Z.R. Hesabi, S.K. Sadrnezhaad, Two-step sintering of nanocrystalline $8Y_2O_3$ stabilized ZrO_2 synthesized by glycine nitrate process, Ceramics International. 35 (2009) 13–20.
[26] X.H. Wang, X.Y. Deng, H.L. Bai, H. Zhou, W.G. Qu, L.T. Li, I.W. Chen, Two-step sintering of ceramics with constant grain-size, II: $BaTiO_3$ and Ni–Cu–Zn ferrite, Journal of the American Ceramic Society 89 (2006) 438–443.
[27] M. Mazaheri, A.M. Zahedi, M. Haghighatzadeh, S.K. Sadrnezhaad, Sintering of titania nanoceramic: densification and grain growth, Ceramics International. 35 (2009) 685–691.
[28] Y.I. Lee, Y.W. Kim, M. Mitomo, D.Y. Kim, Fabrication of dense nanostructured silicon carbide ceramics through two-step sintering, Journal of the American Ceramic Society 86 (2003) 1803–1805.
[29] M. Michálková, K. Ghillányová, D. Galusek, Standard and two-stage sintering of a submicrometer alumina powder: the influence on the Sintering Trajectory, in: R.K. Bordia, E.A. Olevsky (Eds.), Advances in Sintering Science and Technology, 209, John Wiley & Sons Inc., New Jersey, 2010, pp. 421–427.
[30] M.I. Mendelson, Average grain size in polycrystalline ceramics, Journal of the American Ceramic Society 52 (1969) 443–446.
[31] J. Han, P.Q. Mantas, A.M.R. Senos, Densification and grain growth of Al-doped ZnO, Journal of Material Research 16 (2001) 459–468.